Polyhedron 29 (2010) 2991–2998

Contents lists available at ScienceDirect

Polyhedron

journal homepage: www.elsevier.com/locate/poly

Novel bioactive *vic*-dioxime ligand containing piperazine moiety: Synthesis, X-ray crystallographic studies, 2D NMR applications and complexation with Ni(II)

Aytek Yılmaz [a], Bilge Taner [a], Pervin Deveci [a], Aslıhan Yılmaz Obalı [a], Uğur Arslan [b], Ertan Şahin [c], H. İsmet Uçan [a], Emine Özcan [a,*]

[a] Selcuk University, Faculty of Science, Department of Chemistry, Konya, Turkey
[b] Selcuk University, Selcuklu Medical Faculty, Department of Clinical Microbiology, Konya, Turkey
[c] Atatürk University, Faculty of Arts and Sciences, Department of Chemistry, Erzurum, Turkey

ARTICLE INFO

Article history:
Received 6 July 2010
Accepted 7 August 2010
Available online 18 August 2010

Keywords:
vic-Dioxime
Nickel(II) complexes
Piperazine moiety
1D and 2D NMR
Crystal structure
Antimicrobial activity

ABSTRACT

A new *vic*-dioxime ligand bearing an important pharmacophore substituent, *anti*-1-(4-benzylpiperazine-1-yl) phenylglyoxime (LH_2) (Scheme 1), has been synthesized and its nickel(II) complex was obtained by the reaction of $NiCl_2{\cdot}6H_2O$ and the ligand. The characterization of the newly formed compounds was performed by elemental analysis, FT-IR, 1D NMR (^1H, ^{13}C, DEPT), 2D NMR (HMBC), ESI mass-spectrometry, TG/DTA, X-ray crystallography. The antibacterial activity was also studied against *Staphylococcus aureus* ATCC 25923, *Streptococcus mutans* RSHM 676, *Enterococcus faecalis* ATCC 29212, *Lactobacillus acidophilus* RSHM 06029, *Escherichia coli* ATCC 25922, *E. coli* ATCC 35218, *Pseudomonas aeruginosa* ATCC 27853. The antimicrobial test results indicated that all the compounds have mild antibacterial activity against both Gram negative and Gram positive bacterial species.

1. Introduction

vic-Dioximes and their metal complexes constitute a class of compounds which have attracted considerable attention for their rich analytical and electrochemical properties [1,2] and their potential applications in many important chemical processes in the fields of medicine [3], bioorganic systems [4], catalysis [5] and metallurgy [6]. In view of the excellent properties of the *vic*-dioxime ligands, several groups including our own have reported the syntheses and X-ray crystal structure analyses of a series of complexes of these ligands with transition metal ions such as nickel(II), copper(II), cobalt(II), cobalt(III) [7,8]. Although the cobaloximes have acquired an independent research field among the oxime complexes because of their usage as model compounds for the study of vitamin B_{12} coenzyme [9–11], the nickel oximes are also of continuing interest since their first discovery by Tschugaev. Many papers that describe the spectral and the structural properties of nickel oximes [8,12] have appeared in recent years and many analytical procedures such as spectrophotometry [13], thermal decomposition [14], potentiometry using nickel selective electrodes [15], and voltammetry [16–18] have been used to study Ni(II)–oxime complexes. Nickel also finds a place in a variety of thin film materials, often alloyed with other elements as a contact material in semiconductor devices [19].

Like oximes, the chemical properties of piperazine derivatives have been intensively investigated in several research areas because of their versatile metal complexing capabilities [20] and their fundamental pharmacological applications. Piperazines and substituted piperazines are important compounds that exhibit various biological activity ranging from antiemetic to anxiolytic, to opioid agonists, or to bradykinin antagonists [21,22]. Due to the broad pharmacological interest in oxime and piperazine derivatives and their great potential for important applications, attachment of piperazine moiety on a *vic*-dioxime compound can lead to new *vic*-dioxime derivatives with important pharmacological properties (Scheme 1). As an extension of this idea of this present contribution, we have enlarged our work to design and to successfully synthesize a new *vic*-dioxime ligand bearing piperazine moiety and its Ni(II) complex as a new class of synthetic antimicrobial agents a long with their in vitro antimicrobial activity. In this paper, LH_2 and its Ni(II) complex are novel and have been characterized using elemental analysis, FT-IR, 1D NMR (^1H, ^{13}C, DEPT), 2D NMR (HMBC), ESI mass-spectrometry, TG/DTA, X-ray crystallography. To the best of our knowledge, this is the first manuscript which includes synthesis, antibacterial activity and enhanced characterization of LH_2 and its Ni(II) complex.

* Corresponding author. Tel.: +90 332 2233859.
E-mail address: emineozcann@gmail.com (E. Özcan).

0277-5387/$ - see front matter © 2010 Elsevier Ltd. All rights reserved.
doi:10.1016/j.poly.2010.08.006

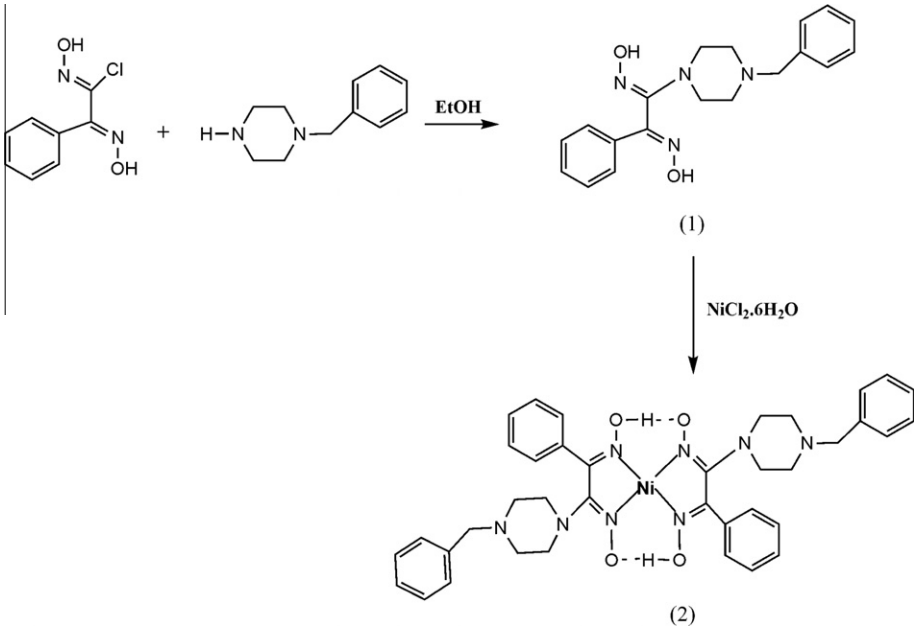

Scheme 1. Routes for the synthesis of the ligand and its Ni(II) complex.

2. Experimental

2.1. Physical measurements

Elemental analyses (C, H, and N) were determined using a LECO-932 CHNSO model analyzer. ^{1}H NMR and ^{13}C NMR spectra were recorded on a Bruker GmbH Dpx-400 MHz High Performance Digital FT-NMR spectrometer with DMSO-d_6 as the solvent with Me_4Si as an internal reference. The IR spectra of solid samples were recorded in a range from 600 to 4000 cm^{-1} on a Perkin–Elmer Spectrum 100 FT-IR spectrometer (Universal/ATR Sampling Accessary). Thermal measurements were carried out on a Setaram Labsys TG–DTA Instruments thermal analysis system in dinitrogen atmospheres, applying a heating rate of 10 °C min^{-1} in a temperature range from 25 to 1073 °C.

2.2. X-ray crystallography

For the crystal structure determination, the single-crystal of the compound LH_2 was used for data collection on a four-circle Rigaku R-AXIS RAPID-S diffractometer (equipped with a two-dimensional area IP detector). The graphite-monochromatized Mo Kα radiation (λ = 0.71073 Å) and oscillation scans technique with $\Delta\omega = 5°$ for each image were used for data collection. The lattice parameters were determined by the least-squares method on the basis of all reflections with $F^2 > 2\sigma(F^2)$. Integration of the intensities, correction for Lorentz and polarization effects and cell refinement were performed using CrystalClear (Rigaku/MSC Inc., 2005) software [23]. The structure was solved by direct methods using SHELXS-97 [24] and refined by a full-matrix least-squares procedure using the program SHELXL-97 [24]. H atoms were positioned geometrically and refined using a riding model. The final difference Fourier maps showed no peaks of chemical significance. Relevant crystal data and details of the structure determinations are given in Table 1.

Crystallographic data (excluding structure factors) for the structures reported in this article have been deposited with the Cambridge Crystallographic Data Center with supplementary publication number CCDC 776609. Copies of the data can be obtained free of charge on application to CCDC, 12 Union Road, Cambridge CB2 1EZ, UK (fax: +44 1223 336 033; e-mail: deposit@ccdc.cam.ac.uk).

Table 1
Crystal data and structure refinement

Empirical formula	$C_{19}H_{22}N_4O_2$
Formula weight	286.4
T (K)	293(2)
Wavelength (Å)	0.71073
Crystal system	Monoclinic
Space group	$P2_1/c$
Unit cell dimensions	
a (Å)	15.1911(4)
b (Å)	5.9128(2)
c (Å)	20.0082(5)
α (°)	90
β (°)	99.329(5)
γ (°)	90
V (Å^3)	719.8(12)
Z	4
D_{calc} (Mg/m^3)	1.27
Absorption coefficient (mm^{-1})	0.085
F(0 0 0)	719.8
θ Range for data collection	2.1–26.4°
Index ranges	$-19 \leqslant h \leqslant 18$, $-6 \leqslant k \leqslant 7$, $-25 \leqslant l \leqslant 25$
Reflections collected	34,255
Independent reflections (R_{int})	3683 (0.167)
Maximum and minimum transmission	0.927 and 0.873
Refinement method	full-matrix least-squares on F^2
Data/parameters	1704/0/228
Goodness-of-fit (GOF)on F^2	0.971
R indices [$F^2 > 2\sigma(F^2)$]	R_1 = 0.065, wR_2 = 0.163
Largest difference in peak and hole (e Å^{-3})	0.201 and −0.213

2.3. Antibacterial activity

The minimal inhibitory concentration (MIC) was determined by broth microdilution methods according to CLSI (Clinical and Laboratory Standards Institute) guidelines (2009) in MHB (Becton Dickinson, Sparks, MD) with an inoculum of approximately 5×10^5 colony-forming units (CFU)/ml. The in vitro antibacterial activity of the compounds was evaluated against standard strains; *Staphylococcus aureus* ATCC (American Type Culture Collection) 25923, *Streptococcus mutans* RSHM 676, *Enterococcus faecalis* ATCC 29212, *Lactobacillus acidophilus* RSHM 06029, *Escherichia coli* ATCC 25922, *E. coli* ATCC 35218, *Pseudomonas aeruginosa* ATCC 27853.

The antibacterial was performed in Mueller–Hinton broth (MHB) (Becton Dickinson, Sparks, MD). All the synthesized compounds were weighed (10.24 mg) and dissolved in DMSO (10 ml) to prepare the stock solutions. The serial dilution from 256 to 0.25 μg/ml was made in a 96-wells plate. To each well 100 μl of a bacterial suspension, obtained from a 24 h culture, containing $\sim 5 \times 10^5$ colony-forming units (CFU)/mL was added. The plate was incubated at 35 °C for 24 h. The data were reported as MICs, the lowest concentration of antibiotics and compounds inhibiting visible growth after 24 h of incubation at 35 °C. For quality control of the method ampicilline (IE Ulugay, Turkey), Genta (IE Ulugay, Turkey) and Piperacilline (Wyeth) were tested as antimicrobial agent. These experiments were carried out in duplicate.

2.4. Synthesis

anti-Chlorophenylglyoxime was synthesized as described [25]. Other reagents purchased from Merck, were reagent grade and were used as received.

2.4.1. Synthesis of the ligand LH_2 (**1**)

1-Benzylpiperazine (0.35 mL, 2 mmol) was dissolved in absolute ethanol (15 mL) and the solution containing *anti*-chlorophenylglyoxime (0.19 g, 1 mmol), in absolute ethanol (20 mL) was added slowly to this solution at room temperature with constant stirring. The reaction mixture was stirred continuously for 3 h at room temperature. Water was added drop-wise until a white precipitate formed. The precipitated ligand was filtered off, washed with cold water, dried and crystallized from water–ethanol (1:3). The ligand is soluble in dichloromethane, ethanol, DMSO and DMF. Yield: 53%. M.p.: 170 °C. *Anal.* Calc. for $C_{19}H_{22}N_4O_2$ (338): C, 67.46; H, 6.51; N, 16.56. Found: C, 67.41; H, 6.49; N, 16.52%. FT-IR (ν_{max}/cm^{-1}): 3233 (O–H), 3033 (Ar–CH), 2947–2807 (CH), 1630 (C=N), 1494 and 1353 (CH), 989 (N–O); MS (EIMS), *m*/*z*: 320 $[M-OH_2]^+$, 291, 103, 77.51; ^1H NMR (DMSO-d_6): δ (ppm) = 11.74 (s, 1H, O–H), 9.24 (s, 1H, O–H), 7.73–7.19 (m, 10H, Ar–H), 3.43 (s, 2H, Ar–CH_2–N), 3.07 (t, 4H, –CH_2–), 2.31 (t, 4H, –CH_2–); ^{13}C NMR (DMSO-d_6): δ (ppm) = 155.52 ($(CH_2)_2$N–C=N–OH), 148.11 (Ar–C=N–OH), 138.54, 131.54, 129.84, 129.73, 129.54, 128.86, 128.72, 127.64 (Ar–C), 62.87 (Ar–CH_2–N), 52.70 (–CH_2–), 46.60 (–CH_2–).

2.4.2. Synthesis of Ni(II) complex (**2**)

An ethanol solution (5 mL) of the $NiCl_2{\cdot}6H_2O$ (0.05 g, 0.21 mmol) was added to an ethanol solution (10 mL) of **1** (0.14 g, 0.42 mmol) while stirring at 50 °C for 15 min. A distinct change in color and a decrease in the pH value (~2) of the solution were observed. Potassium hydroxide (0.42 mmol) in ethanol (20 mL) was added (pH ~6) and the reaction mixture was cooled to room temperature. The red product was precipitated at room temperature and filtered off and then the precipitate that is soluble in common organic solvents such as methanol, dichloromethane and DMSO was washed with cold water. Yield: 78%. M.p.: 238 °C. *Anal.* Calc. for $C_{38}H_{42}N_8O_4Ni$ (732): C, 62.29; H, 5.74; N, 15.30. Found: C, 62.22; H, 5.81; N, 15.25%. FT-IR (ν_{max}/cm^{-1}): 3036 (Ar–CH), 2942–2819 (CH), 1770 (O–H···O), 1567 (C=N), 1494 and 1389 (CH), 1004 (N–O); ^1H NMR (DMSO-d_6): δ (ppm) = 16.06 (s, 2H, O–H···O), 7.43–7.18 (m, 20H, Ar–H), 3.27 (s, 4H, Ar–CH_2–N), 2.97 (t, 8H, –CH_2–), 2.15 (t, 8H, –CH_2–); ^{13}C NMR (DMSO-d_6): δ (ppm) = 152.45 ($(CH_2)_2$N–C=N–OH), 145.21 Ar–C=N–OH, 138.39, 131.51, 129.98, 129.80, 129.43, 128.81, 128.52, 127.61 (Ar–C), 62.59 (Ar–CH_2–N), 52.96 (–CH_2–), 49.19 (–CH_2–).

3. Results and discussion

3.1. Crystal structure of ligand

The X-ray structure of the ligand was determined in order to confirm the assigned structure and to establish conformation of the molecule. ORTEP drawing of the structure with atomic numbering is shown in Fig. 1, and the selected geometric parameters are given in Table 2. Ligand crystallizes in the monoclinic space group $P2_1/c$ with four molecules in the unit cell. The asymmetric unit contains one molecule. The molecular structure was formed

Table 2
Selected bond lengths (Å) and angles (°), and hydrogen bonds for the ligand.

Bond lengths			
N2–C9	1.462(4)	N2–C12	1.405(4)
N3–C12	1.276(5)	N1–C11	1.469(5)
N4–C13	1.278(5)	N3–O2	1.412(4)
N1–C7	1.479(4)	C6–C7	1.504(4)
Bond angles			
C9–N2–C12	115.3(3)	N4–C13–C14	128.5(3)
N4–C13–C12	110.0(3)	C14–C13–C12	121.4(3)
C6–C7–N1	120.8(4)	O1–N4–C13	113.4(4)
Hydrogen bonds			
D–H···A	d(H···A)	d(D···A)	<(DHA)
O1–H···N2[a]	0.82	3.229(4)	154
O1–H···N4[a]	0.82	2.837(5)	132
O2–H···N1[b]	0.82	2.858(4)	171

[a] Symmetry transformations used to generate equivalent atoms: $-x, 2-y, -z$.
[b] Symmetry transformations used to generate equivalent atoms: $-x, 1/2+y, 1/2-z$.

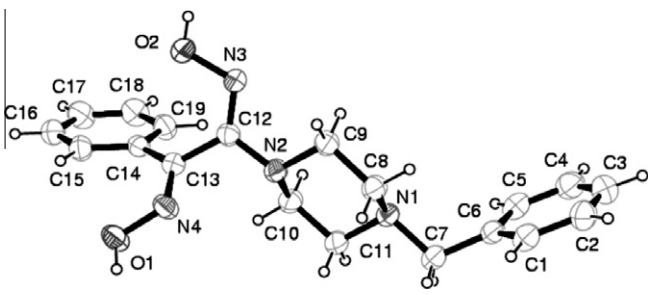

Fig. 1. The molecular structure of the ligand showing the atom numbering scheme. The thermal ellipsoids are plotted at the 40% probability level.

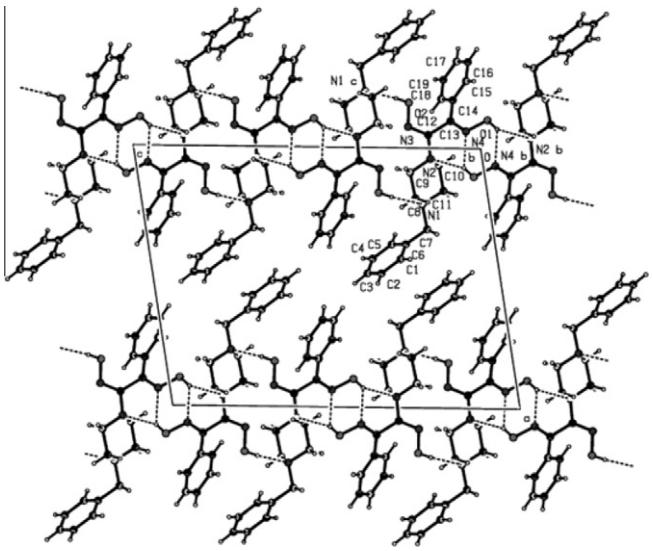

Fig. 2. Packing diagram with the *H*-bonding geometry of ligand down the *b*-axis.

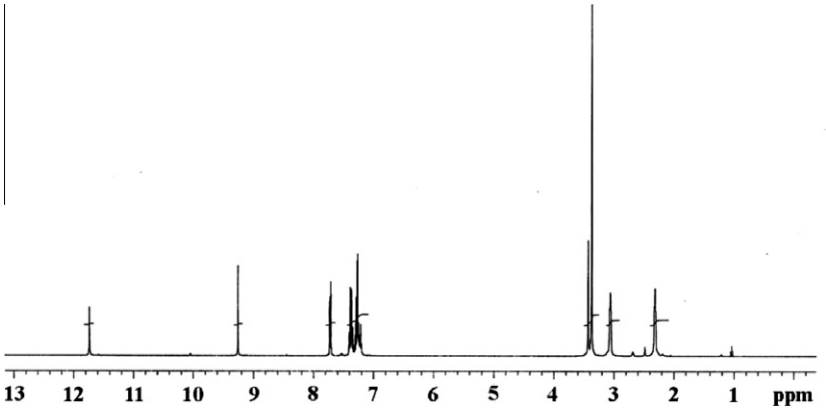

Fig. 3. ^{1}H NMR spectrum of ligand in DMSO-d_6 at 25 °C (400 MHz).

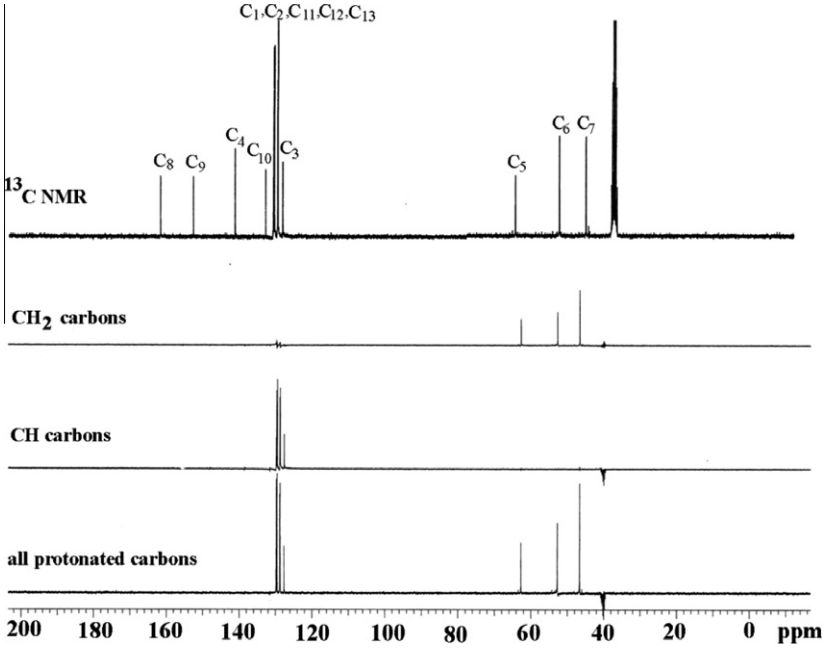

Fig. 4. The ^{13}C NMR and DEPT spectra of ligand.

by combining phenyl, ethanedial dioxime, piperazine and benzyl groups respectively. As expected, the phenyl moieties are planar. The dihedral angles between the mean planes of two phenyl rings are 21.7(1)°. Piperazine (N1/C8/C9/N2/C10/C11) ring adopts the chair conformation. The puckering parameters of this ring are $Q = 0.583(3)$ Å, $\theta = 176.5(3)°$, $\Phi = 184(5)°$ [26]. N1 and N2 atoms are displaced from the C8/C9/C10/C11 mean plane by 0.340(2) and −0.306(2) Å. Piperazine itself has the ideal chair conformation with N–H bonds in the equatorial positions [27]. The glyoxime moiety is not planar and the bond lengths in the oxime group are in harmony with the values in the previously solved structure [28]. Oxime groups possess stronger hydrogen-bonding capabilities than alcohols, phenols and carboxylic acids [29]. The hydrogen-bond systems in the crystals of oximes have been analyzed and a correlation between a pattern of hydrogen-bonding and N–O bond lengths have been suggested [30]. In parallel, hydrogen bonds are the main driving forces for oxime non-covalent interactions and *oxime functionality* can be stereoelectronically adjusted for precise directed assembly of homomeric intermolecular oxime···oxime and oxime···N–heterocycle molecular motifs [31]. Our compound formed a head-to-head $R_2^2(6)$ motif as well, which is the characteristic six-membered ring arrangement in oximes, resulting in classical oxime dimmers. With the other oxime group, the crystal structure of the ligand formed an oxime···N (piperazine) motif that generated an infinite chain which is parallel to the *c*-axis (Fig. 2).

3.2. FT-IR analysis of ligand and its Ni(II)complex

In the IR spectrum of ligand, the strong ν(OH), ν(C=N) and ν(NO) characteristic stretching vibrations bands were observed at 3233, 1630, and 989 cm^{-1}, respectively. In the IR spectrum of Ni(II) complex, disappearance of the sharp intense ν(–NOH) stretching vibration band at 3233 cm^{-1}. The IR spectra of complex showed a weak deformation band at ca. 1770 cm^{-1}, indicative of intramolecular hydrogen bonded bending vibrations (O–H···O) associated with the square-planar *vic*-dioxime complexes. As ν(NO) stretching vibrations of ligand shift to slightly higher frequencies, the ν(C=N) stretching vibrations shift to slightly lower frequencies, and it indicates the coordination of the azomethine nitrogen to the metal center. Yuksel et al. [8] showed that *vic*-dioxime ligand form square-planar Ni(II) complex in which the ligands chelate via nitro-

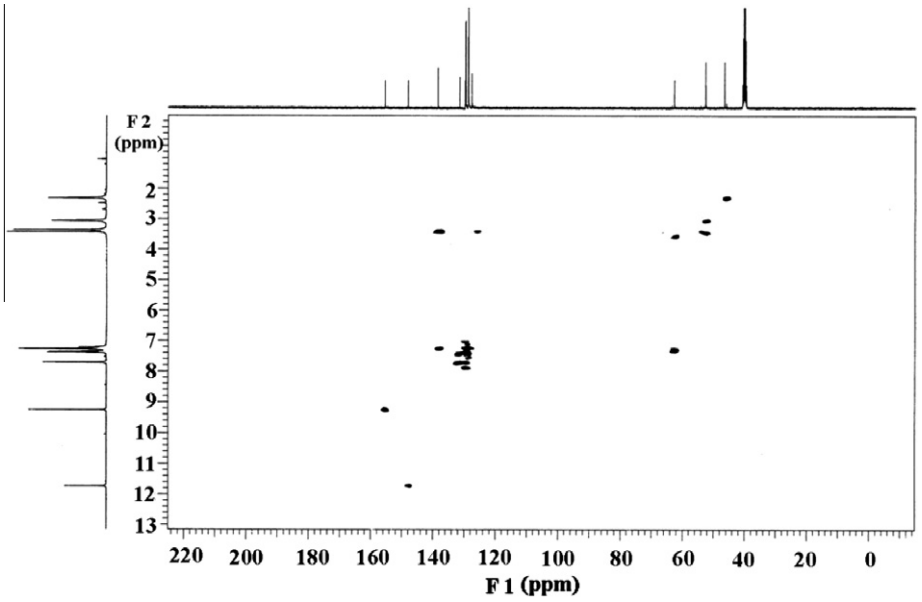

Fig. 5. 2D HMBC spectrum of ligand.

Table 3
^{13}C NMR, DEPT and HMBC spectral data and assignments.

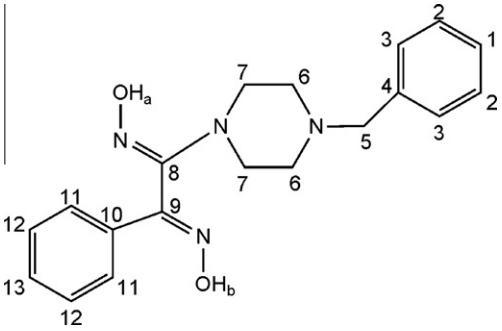

Chemical shifts	DEPT	HMBC	Assignments
155.52	C	9.24	C_8
148.11	C	11.74	C_9
138.54	C	7.40, 3.43	C_4
131.54	C	7.70, 7.37	C_{10}
129.84–128.72	CH	7.19–7.73	C_{11}, C_{13}, C_2, C_1,C_{12}
127.64	CH	7.25, 3.43	C_3
62.87	CH_2	7.25, 3.07	C_5
52.70	CH_2	3.43, 3.07	C_6
46.60	CH_2	2.31	C_7

gen and oxygen donor atoms. IR band in 510 cm^{-1} region was attributed to (Ni–N). The FT-IR spectra of the compounds exhibited two medium intensity absorption signals at between 3000 and 3100 cm^{-1} result from phenyl group. Additionally, the strong and very strong CH_2 stretching bands were observed at 2944 and 2824 cm^{-1}.

In order to study the binding properties of the dioxime ligand and the metal ion in complex, the IR spectrum of the free oxime ligand is compared to the Ni(II) complex. In the IR spectrum of the ligand, O–H stretching vibration is observed at 3233 cm^{-1} as a broad absorption band. C=N and N–O stretching vibrations are obtained at 1630 and 989 cm^{-1} respectively. In the IR spectrum of Ni(II) complex, disappearance of the sharp intense ν(–NOH) stretching vibration band at 3233 cm^{-1}, shift in the ν(C=N) stretching band to lower

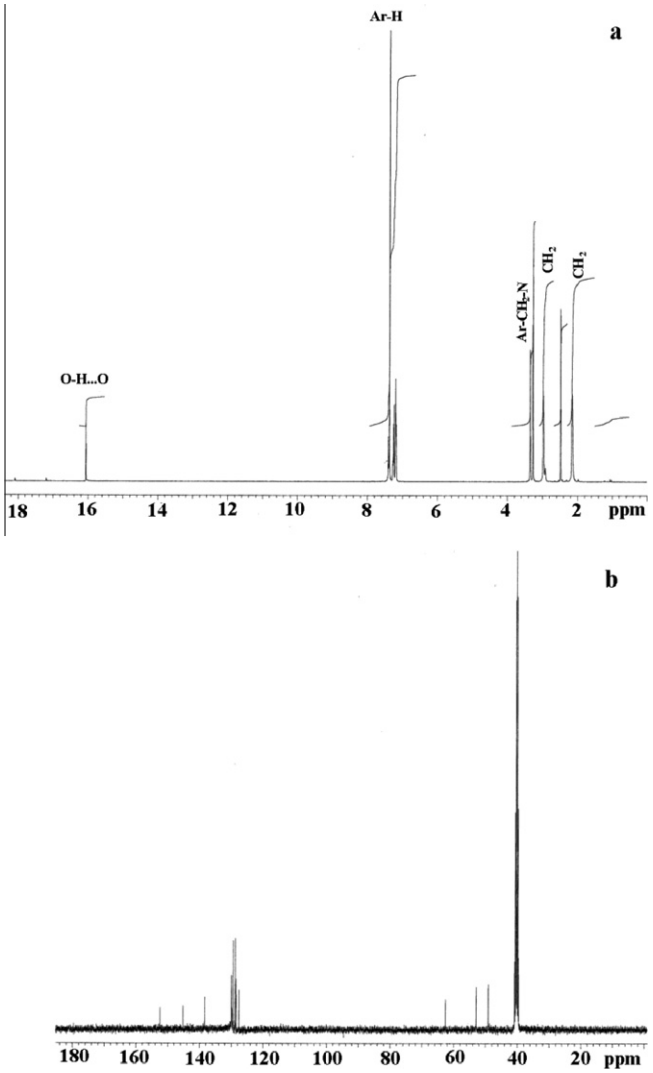

Fig. 6. The Ni(II) complex of (a) ^{1}H NMR spectrum and (b) ^{13}C NMR spectrum.

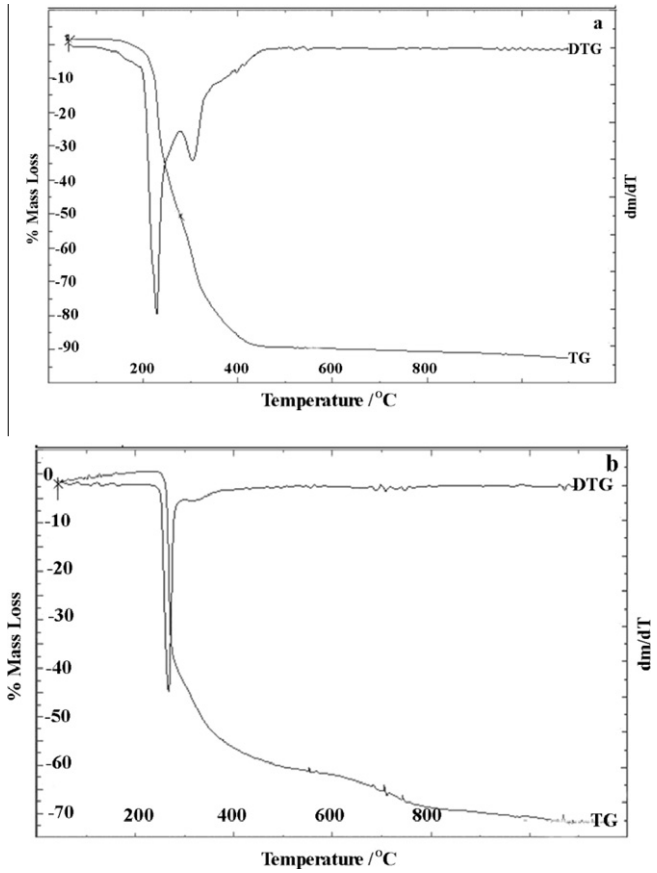

Fig. 7. TG/DTG diagram of (a) ligand and (b) Ni(II) complex.

frequency, and the appearance of the broad O–H···O deformation vibration at ca. 1770 cm^{-1} are indicative of formation of complex and N,N′-chelation in this complex [8].

3.3. NMR characterizations

3.3.1. ^1H, ^{13}C NMR, DEPT and HMBC spectrum of ligand

In the ^1H NMR spectrum of LH_2 in DMSO-d_6, the deuterium exchangeable protons of the =N–OH groups show chemical shifts at 11.74 and 9.24 ppm as singlets which indicate an (E; E)-structure for the *vic*-dioxime [32]. The chemical shifts which belong to –CH_2 protons (Ar–CH_2–N) are observed at 3.43 ppm as a singlet while the other –CH_2 protons are observed at 2.31 and 3.07 ppm as a triplet. Aromatic protons in the structure are also observed at 7.19–7.73 ppm as a multiplet. (Fig. 3).

^{13}C NMR spectrum shows 13 different carbon atoms which are consistent with the proposed structure of ligand on the basis of molecular symmetry. In the ^{13}C NMR, carbon resonances of hydroxyimino groups (–C=N–OH) are observed at 155.52 and 148.11 ppm as expected for *vic*-dioximes [8]. Distortionless enhancement of NMR signals by polarization transfer (DEPT) is used to discriminate better different types of carbons present in ligand. The DEPT spectrum (Fig. 4) gives the CH_2 peaks at 46.60, 52.70, 62.87 ppm and the CH peaks at 127.64, 128.72, 128.86, 129.54, 129.73, 129.84 ppm. The carbons recorded in ^{13}C NMR but are nulled in DEPT are carbons without any attached hydrogens.

More detailed information about the structure of ligand is provided by 2D HMBC spectrum (Fig. 5) and specific assignments of protons and carbons are made as follows (Table 3).

The HMBC spectrum (Fig. 5) shows that H_a and H_b protons exhibit long range coupling with hydroxyimino carbons at 155.52 (C_8) and 148.11 (C_9) ppm, respectively. Other correlations are also in accordance with the proposed structure (Table 3).

3.3.2. ^1H and ^{13}C NMR spectrum of the Ni(II) complex

^1H NMR spectrum of the *vic*-dioxime complexes can be evaluated to determine the isomer formed, since the various chemical environments show two O–H···O bridge protons in the cis-form, only one of which is in the trans-structure [33]. In the ^1H NMR spectrum of Ni(II) complex (Fig. 6a), the resonance of intramolecular bonding (O–H···O) protons are observed at 16.06 ppm, which disappear by D_2O exchange. Since only one signal occurs at 16.06 ppm for the complex, the trans-form of this complex is confirmed (Scheme 1). This is in agreement with similar *vic*-dioxime complexes in the literatures [9,10,34,35]. In the ^{13}C NMR spectra (Fig. 6b), quaternary carbon signals of the hydroxyiminocarbon (C=N–O) appeared at 152.45 and 145.21 ppm. The other chemical shifts (^1H- and ^{13}C NMR) observed for complex are very similar to those which are found for ligand.

3.4. Thermal analysis

The synthesized *vic*-dioxime ligand melts at 170–171 °C with simultaneous decomposition. The first mass loss was observed at 174 °C in the TG profile. The TG/DTG profiles of the ligand are shown in Fig. 7a. From the TG curve, it appeared that the sample

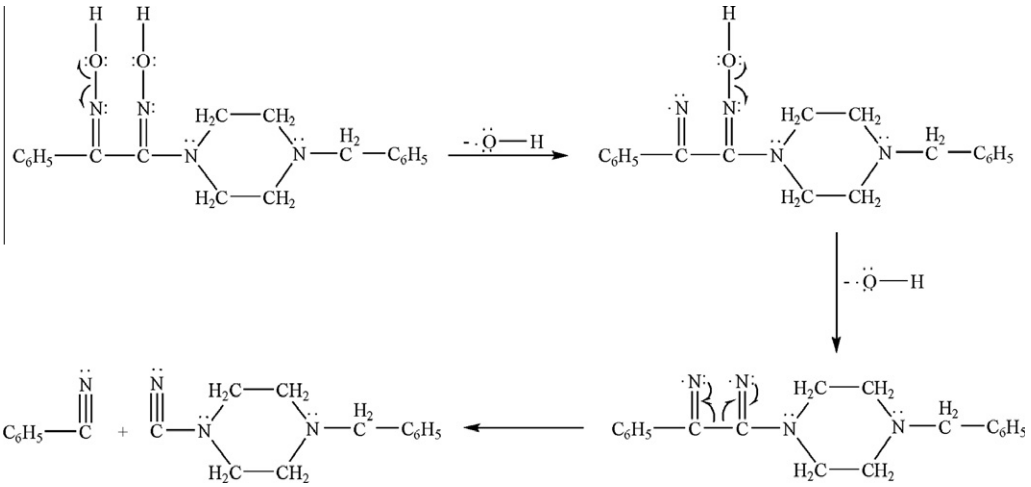

Scheme 2. Mechanism of decomposition of LH_2.

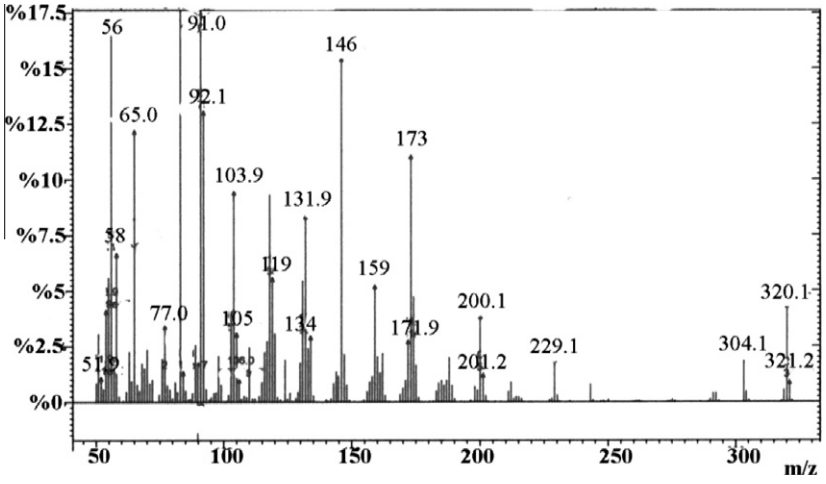

Fig. 8. GC–MS spectrum of ligand.

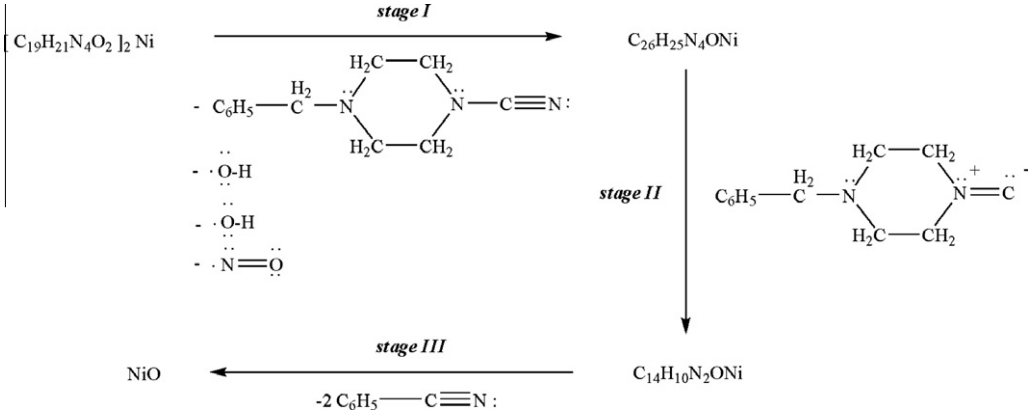

Scheme 3. Decomposition of Ni(II) complex.

Table 4
Antibacterial activities of LH_2 and its Ni(II) complex as MIC values (μg/ml).

	S. mutans RSHM 676	*E. faecalis* ATCC 29212	*L. acidophilus* RSHM 06029	*S. aureus* ATCC 25923	*E. coli* ATCC 35218	*E. coli* ATCC 25922	*P. aeruginosa* ATCC 27853
Piperacilline	4	2	0,5	2	4	2	2
Ampicilline	32	64	16	0,5	128	128	128
Gentamycin	0,5	2	2	1	0,5	1	0,5
LH_2	256	64	32	128	64	64	128
Ni(II) complex	128	64	32	128	128	128	128

decomposes in two stages over the temperature range 25–800 °C The first decomposition occurs between 174 and 314 °C with a mass loss of 69.7% (calculated 69.5%) and the second decomposition starts at 314 °C and ends at 800 °C with a 30.2% (calculated 30.5%) mass loss.

Mechanism of decomposition for the ligand is possible as shown by Scheme 2. The theoretical mechanism given in Scheme 2 is in agreement with that of Burakevich et al. [25], who studied with phenylglyoxime in 1971. The theoretical mechanism dealt with in Scheme 2 is confirmed by the GC–MS data in Fig. 8. The peaks observed at 321, 303, 201, 103, 77, 51 *m*/*z* are responsible for the evolved radical moiety. The molecular ion is not detected in the mass spectra of the ligand, probably due to this high thermal instability in the ionization beam.

The TGA curve of the Ni(II) complex shows three stages of decomposition within the temperature range of 25–900 °C (Fig. 7b). The complex shows no mass loss up to 235 °C, indicating the absence of water or other adsorptive molecules. The first decomposition occurs between 235 and 278 °C with 35.7% (calculated 35.8%) mass loss, the second decomposition occurs between 285 and 410 °C with 24.9% (calculated 25.6%) mass loss and the third decomposition occurs between 486 and 900 °C with 28.3% (calculated 28.1%) mass loss. The mass losses found experimentally are very close to the theoretical values.

From these results it was found that the Ni(II) complex was converted to the corresponding NiO as shown in Scheme 3 [14,36–38]. The oxide yielded at the end of pyrolysis was confirmed by TG/DTG data given in Fig. 7b.

3.5. Biological activity

The synthesized *vic*-dioxime ligand and its Ni(II) complex exhibited highest antimicrobial activity against *S. aureus*, *S. mutans*, *E. faecalis*, *L. acidophilus*, *E.* coli ATCC 25922, *E. coli* ATCC 35218 and

P. aeruginosa in 128, 256, 64, 32, 64, 64, 128 and 128, 128, 64, 32, 128, 128, 128 μg/ml concentrations respectively (Table 4). A comparative study of MIC values of the ligand and its Ni(II) complex indicates that the free ligand has a better activity than has the metal complex against *E. coli* and LH_2 exhibited antibacterial activity in 64 μg/ml concentration, whereas the antibacterial activity of Ni(II) complex was observed in 128 μg/ml MIC value against *E. coli*. However, Ni(II) complex shows high bactericidal activity against *S. mutans* (MIC = 128 μg/ml) as compared to free ligand. Both of the compounds have same MIC values against test microorganisms for *S. aureus*, *E. faecalis*, *L. acidophilus*, and *P. aeruginosa*. The present investigations of antimicrobial screening data revealed that the newly synthesized compounds exhibited mild activity compared to that of the control drugs. Moreover, we will synthesize novel piperazine moiety compounds, and try our best to discover their structure–activity relationships.

4. Conclusions

We have described the preparation, characterization and biological activities of a novel *vic*-dioxime ligand and its Ni(II) metal complex which were substituted peripherally with bioactive piperazine moiety. The spectroscopic analysis confirmed the composition and the structure of the newly obtained compounds. It was concluded from TG/DTG studies that the thermal stability of the Ni(II) complex is higher than that of the ligand since the free =C=NOH groups in the ligand participate in some internal redox decomposition processes. The antibacterial data given for the compounds presented in this paper allowed us to state that the *vic*-dioxime ligand generally has a better activity than the Ni(II) complex and all the compounds have mild antibacterial activity against both Gram negative and Gram positive bacterial species.

References

[1] P. Rodríguez, E. Herrero, J. Solla-Gullón, J.M. Feliu, A. Aldaz, J. Solid State Electrochem. 12 (2008) 575.
[2] L. Husáková, A. Bobrowski, J. Šrámková, A. Krôlicka, K. Vytras, Talanta 66 (2005) 999.
[3] L. Musılova, K. Kuca, Y.S. Jung, D. Jun, Clin. Toxicol. 47 (2009) 545.
[4] A. Mokhir, R. Krämer, Y.Z. Voloshin, O.A. Varzatskii, Bioorg. Med. Chem. Lett. 14 (2004) 2927.
[5] B.G. Malmstrom, Acc. Chem. Res. 26 (1993) 332.
[6] L.O. Filippov, R. Joussemet, R. Houot, Miner. Eng. 13 (2000) 37.
[7] A.V. Makarycheva-Mikhailova, P.V. Gushchin, M.N. Kopylovich, I.N. Ganebnykh, V.N. Charushin, M. Haukka, A.J.L. Pombeiro, V.Yu. Kukushkin, Inorg. Chem. Commun. 9 (2006) 869.
[8] F. Yuksel, A.G. Gürek, M. Durmuş, İ. Gürol, V. Ahsen, E. Jeanneau, D. Luneau, Inorg. Chim. Acta 361 (2008) 2225.
[9] D. Mandal, B.D. Gupta, Organometallics 25 (2006) 3305.
[10] M. Bhuyan, M. Laskar, B.D. Gupta, Organometallics 27 (2008) 594.
[11] V. Vijaikanth, B.D. Gupta, D. Mandal, S. Shekhar, Organometallics 24 (2005) 4454.
[12] O. Pantani, E. Anxolabéhére-Mallart, A. Aukauloo, P. Millet, Electrochem. Commun. 9 (2007) 54.
[13] S. Karaböcek, S. Nohut, S. Güner, Anal. Chim. Acta 408 (2000) 163.
[14] H. Arslan, N. Özpozan, N. Tarkan, Thermochim. Acta 383 (2002) 69.
[15] B. Pihlar, P. Valenta, H.W. Nurnberg, Z. Fresenius, Anal. Chem. 307 (1981) 337.
[16] J.R. Donat, K.W. Bruland, Anal. Chem. 60 (1988) 240.
[17] J. Golimowski, A. Tykarska, J. Fresenius, Anal. Chem. 349 (1994) 620.
[18] W.R. Jin, V.D. Nguyen, P. Valenta, H.W. Nurnberg, Anal. Lett. 30 (1997) 1235.
[19] M.P. Hogan, K.A. Abboud, K.H. Dahmen, Chem. Mater. 10 (1998) 2525.
[20] H.J. Schneider, Angew. Chem., Int. Ed. Engl. 30 (1991) 1417.
[21] E. Mishani, C.S. Dence, T.J. McCarthy, M.J. Welch, Tetrahedron Lett. 37 (1996) 319.
[22] P. Chaudhary, R. Kumar, A.K. Verma, D. Singh, V. Yadav, A.K. Chhillar, G.L. Sharma, R. Chandra, Bioorg. Med. Chem. 14 (2006) 1819.
[23] Rigaku/MSC, Inc., 9009 New Trails Drive, The Woodlands, TX 77381.
[24] G.M. Sheldrick, SHELXS97 and SHELXL97, University of Göttingen, Germany, 1997.
[25] J.V. Burakevich, A.M. Lore, G.P. Volpp, J. Org. Chem. 36 (1971) 1.
[26] D. Cremer, J.A. Pople, J. Am. Chem. Soc. 97 (1975) 1354.
[27] A. Parkin, Acta Crystallogr. B60 (2004) 219.
[28] Y. Köysal, S. Isik, N. Sarikavakli, F. Erduran, Acta Crystallogr. E60 (2004) 515.
[29] A.W. Marsman, E.D. Leussing, J.W. Zwikker, L.W. Jenneskens, Chem. Mater. 11 (1999) 1484.
[30] V. Bertolasi, G. Gilli, A.C. Veronese, Acta Crystallogr. B38 (1982) 502.
[31] E. Alcalde, N. Mesquida, C. Alvarez-Rúa, R. Cuberes, J. Frigola, S. García-Granda, Molecules 13 (2008) 301.
[32] M. Kurtoğlu, E. Ispir, N. Kurtoğlu, S. Serin, Dyes Pigments 77 (2008) 75.
[33] A. Coşkun, F. Yılmaz, E.G. Akgemici, J. Inc. Pheo. Chem. 60 (2008) 393.
[34] P. Deveci, E. Özcan, B. Taner, O. Arslan, J. Coord. Chem. 61 (2008) 857.
[35] B.D. Gupta, R. Yamuna, D. Mandal, Organometallics 25 (2006) 706.
[36] M.L. Kantouri, A. Hatzidimitriou, M. Udin, Polyhedron 18 (1999) 3441.
[37] Cs. Varhelyi Jr., G. Pokol, Á. Gömöry, A. Ganescu, P. Sohar, G. Liptay, Cs. Varhelyi, J. Therm. Anal. Calorim. 83 (2006) 701.
[38] D. Atılla, S. Asma, A.G. Gurek, J. Coord. Chem. 18 (2009) 3050.